Ion fluence dependence of the Si sputtering yield by noble gas ion bombardment

A. Mutzke, W. Eckstein

Max-Planck-Institut für Plasmaphysik, EURATOM Association,

D-17491 Greifswald, Germany,

D-85748 Garching bei München, Germany

Abstract

The effect of sputtering yield enhancement by implantation of noble gases into solid silicon is investigated with the Monte Carlo program SDTrimSP. The process of diffusion is incorporated into the program to describe the outgassing of noble gases. The bombardment of Si with He, Ne, Ar, Xe at normal incidence is studied in the energy range from 1 to 500 keV. Good agreement of the calculated results with experimental data is found.

Key words: Atoms scattering, Atoms sputtering, atom, molecule, ion impact, applications of Monte Carlo method, Numerical methods, film deposition,

PACS: 34.50, 79.20.R, 02.50.U, 02.60, 81.15.C,

1 Introduction

The sputtering yield is often determined experimentally by the weight-change method, where the mass of the removed material is measured by weighing the target before and after bombardment. Due to the limited sensitivity of the balance a large fluence of incident particles has to be applied. This leads to the measurement of a so-called steady state sputtering yield, which may differ from the yield of the pure material due to the implantation of the bombarding species in the target. For nonvolatile species like metal ions this can lead to a completely changed target composition [1] and dramatic effects like oscillations in the sputtering yield with increasing fluence [2]. For noble gas ions the implantation of these species is usually regarded to be small. The influence of the implanted ions on the sputtering yield depends on the ratio of ion mass to target mass, but also on the depth distribution of the implanted atoms and their maximum atomic fraction in the target. Therefore, the sputtering yield should change with fluence until steady state is reached. Blank and Wittmaack [3] have shown this effect for the bombardment of Si with 140 keV Xe. They found an increase of the sputtering yield of about 20% due to the increased scattering of the implanted Xe. They also determined the total implanted Xe by Rutherford scattering but not a depth distribution.

The purpose of this paper is to go a step further to provide information of the depth distribution and maximum atomic fraction of the implanted Xe de-

pendent on the incident energy. Furthermore, the dependence on the incident species or mass ratio is investigated. Computer simulation is applied for these studies.

2 Simulation

The calculations were performed with the Monte Carlo program SDTrimSP [4], which is a new version of TRIM.SP [5,6]. This advanced version has included all aspects of earlier developments, allows the use of different interaction potentials, different integration schemes, time development as well as static and dynamic calculations. SDTrimSP can run on sequential and parallel architectures.

The implantation of gas atoms in the target changes the density as a function of depth and the scattering behaviour inside the solid, and has, therefore, an influence on the collision cascade on the depth profile and on sputtering.

The gas atoms are handled in the usual way, but due to their low binding energy (nearly zero for noble gases) they can more easily be sputtered. This leads to the result that the gas concentration near the surface (depth smaller than the mean range of the implanted ions) is lower than in deeper layers.

The effect of outgassing in the former program TRIDYN was realised by the reemission of atoms, namely the removal of atoms from the target without any

transport of these atoms through the surface. In this case the knowledge of the maximum atomic fraction of the noble gas content in the solid is required for their removal.

One possibility of gas transport in the solid is diffusion. The diffusion flux, J, through a surface with a diffusion-coefficient, D, is:

$$J = -D \cdot \frac{\partial c}{\partial x} \tag{1}$$

where c is gas impurity concentration and x the depth. The time dependent change of the concentration is:

$$\frac{\partial c}{\partial t} = -D \cdot \frac{\partial^2 c}{\partial x^2} \tag{2}$$

Another alternative is the direct transport of gas driven from the pressure and density respectively.

The outgasing flux, J, through a surface with a transport coefficient, K, is:

$$J = -K \cdot c \tag{3}$$

and the corresponding time dependence of the concentration:

$$\frac{\partial c}{\partial t} = -K \cdot \frac{\partial c}{\partial x} \tag{4}$$

A time dependence is simulated by a fluence dependence. At each fluence step a certain amount of gas atoms is moved to the upper layer (in direction to the surface). The amount is dependent on the concentration c of gas atoms (atoms

per volume) in the layer and an outgassing coefficient K. This coefficient can be determined by a comparison with experimental data.

3 Results

The best experimentally documented system is the case of Xe bombardment of Si [3]. This example will be discussed below in more detail. At 140 keV, Xe is deposited at larger depths at zero than at increasing Xe fluence due to the larger scattering of Xe compared with Si. The reflection of Xe is negligible, because the particle reflection coefficient is nearly zero at low fluences and increases to the order of 10^{-4} at steady state.

For a better understanding of the influence of the diffusion and/or outgassing process three examples are considered: 1) no diffusion and no outgassing, $D = 0$, $K = 0$, 2) no diffusion, $D = 0$, $K = K_s$, and 3) no outgassing, $D = D_s$, $K = 0$. The coefficients K_s and D_s for Xe

$$K_s(Xe) = 100 \cdot 10^{24}\ cm^3/ion \tag{5}$$
$$D_s(Xe) = 20 \cdot 10^{36}\ cm^4/ion \tag{6}$$

were determined by a comparison with experimental steady state data (the reason for the subscript s in K_s and D_s), see Fig. 1. For 140 keV Xe into Si K_s was determined in such a way, that the areal density at steady state is equal to the experimental result. For He, Ne, and Ar the determination of K_s was performed according to the equation

$$K_s(x) = K_s(Xe) \cdot \frac{density(x)}{density(Xe)} \tag{7}$$

with x = He, Ne, Ar.

Measurements of the areal densities at steady state at different incident energies justify the procedure of the K_s determination for Xe and Ar; for He and Ne the same procedure is assumed to be correct.

The calculated values for the areal density of the implanted Xe show exactly the same result as in [3], see Fig. 1, for the case of negligible diffusion, $D = 0$ and $K = K_s \neq 0$, whereas the other two examples do not agree with the experimental findings. This result is expected since the diffusion of Xe in Si is regarded to be small. An interesting point is the occurrence of a maximum in the areal density at a fluence of about $7 \cdot 10^{16}$ atoms/cm^2.

The calculated results for the sputtering yield show good agreement with the experimental values [3], see Fig. 2, for the same case of negligible diffusion as in Fig. 1. The increased scattering in the Si target due to the Xe implantation leads to an increase in the sputtering yield of Si with increasing fluence as reported in [3]. There remains a difference between calculated results and the experimental data at low fluences. Because of the small atomic fraction of Xe near the surface at low fluence ($2 \cdot 10^{16}$ atoms/cm^2) it is very likely, that the Si partial yield should start with a zero slope at low fluence. This is also supported by the fact that the sputtering of Xe stays nearly zero until a fluence of about $2 \cdot 10^{16}$ atoms/cm^2. At steady state the partial yield of Xe reaches

unity but this amounts to about 25% of the partial yield of Si. At a fluence of about $9 \cdot 10^{16}$ atoms/cm^2 the Xe partial sputtering yield shows a slight maximum above unity.

Regarding the depth profiles of the implanted Xe, the incident ions are deposited at large depths with a maximum at about 65 nm at a low fluence ($2 \cdot 10^{16}$ atoms/cm^2) and nearly no Xe atoms close to the surface, as shown in Fig. 3. With increasing fluence the profile becomes more asymmetric and moves toward the surface due to the erosion of the Si target and the increased scattering caused by the implanted Xe. The integrals over these profiles give the values in Fig. 1. Finally a steady state profile is reached at $1.5 \cdot 10^{17}$ atoms/cm^2. The maximum of the Xe areal density in Fig. 1 can be explained by a change in the Xe profile in the first 50 nm, see Fig. 3 at $9 \cdot 10^{16}$ atoms/cm^2. There occurs a rearrangement around the maximum of the profile. The Xe atomic fraction near the surface (< 10 nm) is proportional to Xe partial sputtering yield.

In Fig. 4 the sputtered depth for the bombardment of Si with 140 keV Xe at normal incidence is plotted versus the incident fluence. Whereas in [3] a linear relation between the sputtered depth and the fluence is assumed, the calculated results clearly demonstrate that at fluences below steady state the surface recession is not linear because of the implantation of Xe.

The fluence to reach steady state or equilibrium, f_{eq}, depends on the incident

energy. At 10 keV equilibrium is reached at a fluence of $2 \cdot 10^{16}$ atoms/cm^2, at 270 keV the fluence needed is about an order of magnitude larger. This agrees very well with the formula, $f_{eq} = \rho R/Y$, proposed in [7], where ρ is the target density, R the mean range of the implanted species, and Y the sputtering yield. It is interesting to note that the maximum in the areal density occurs at all energies, see Fig. 5, but with the smallest effect at low energies.

Switching to the other nobel gases as bombarding species it is assumed as a first estimate, that the outgasing coefficient, K, for Ar, Ne and He is assumed to be inversely proportional to the liquid gas density, see Fig. 6. The comparison of experimental and calculated steady state areal densities supports the choice of the outgassing factors as can be seen in the results.

Also a comparison of experimental and calculated steady state Si sputtering yields versus the incident energy is satisfactory for Xe as well as Ar bombardment of Si at normal incidence, as demonstrated in Fig. 7. Similar agreement is found for the areal densities, see Fig. 8. It should be mentioned that some experiments were performed at an angle of incidence at 15° instead of normal incidence. Calculations have shown, that the results at 15° deviate somewhat from the results at normal incidence, but these deviations are mostly within the error limits of the experiment.

With the same calculation procedure, the steady state Si sputtering yields are determined for He, Ne, Ar and Xe and compared to experimental data in Fig.

9. The simulations for Ne, Ar and Xe computed with negligible diffusion. The diffusion-coefficient for He is

$$D_s(He) = 5000 \cdot 10^{32}\ cm^4/ion\ . \tag{8}$$

The agreement between experimental data and calculated results is again satisfactory, but the question remains how the steady state is reached for the different ion species.

The implantation of a heavy element like Xe into a target consisting of a light element will decrease the implantation range and increase the scattering inside the target, which will lead to an increase in sputtering. The opposite effect is expected for light ion implantion into a heavier matrix. The calculated fluence dependences of He, Ne, Ar and Xe implanted into Si clearly demonstrate this behaviour, as shown in Fig. 10. For Ar there is still an increase in Si sputtering yield but lower than for Xe, whereas for Ne the effect is negligible. For He there appears indeed a reduction in the Si sputtering yield with the incident fluence as expected.

From the depth profiles of the implanted noble gases the maximum atomic fractions of these species in Si have been determined dependent on the incident energy at normal incidence. Fig. 11 shows that for the lighter ions the atomic fraction is increasing with energy in the energy range from 0.1 to 10 keV, whereas it decreases for Xe.

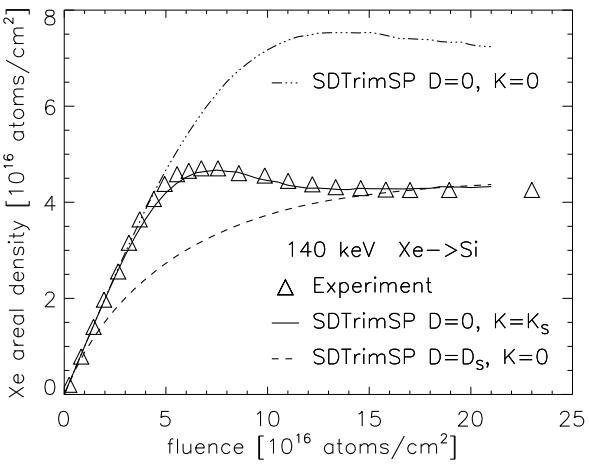

Fig. 1. Calculated areal density of implanted Xe versus the incident fluence compared with experimental data [3]. Si is bombarded with 140 keV Xe at normal incidence

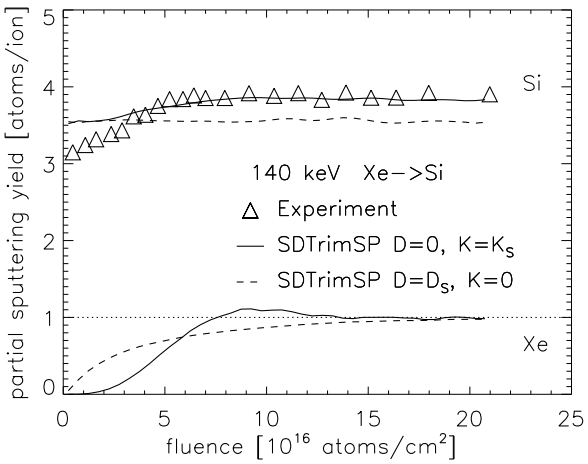

Fig. 2. Calculated total and partial sputtering yields of Si and Xe versus the incident fluence of 140 keV Xe on a Si target at normal incidence compared with experimental data [3]

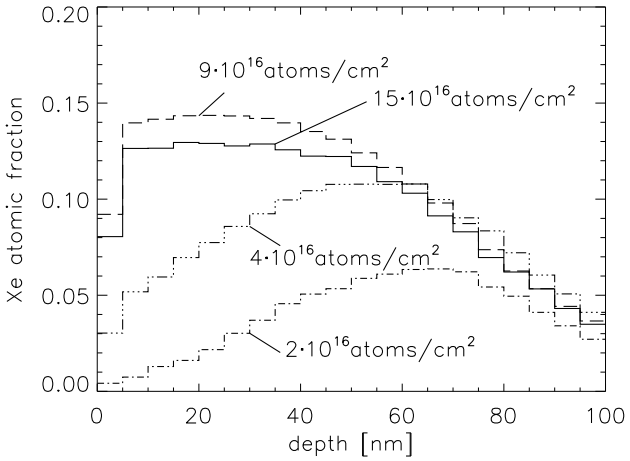

Fig. 3. Calculated depth profiles of the implanted Xe for the bombardment of Si with 140 keV Xe at normal incidence with varying incident Xe fluence

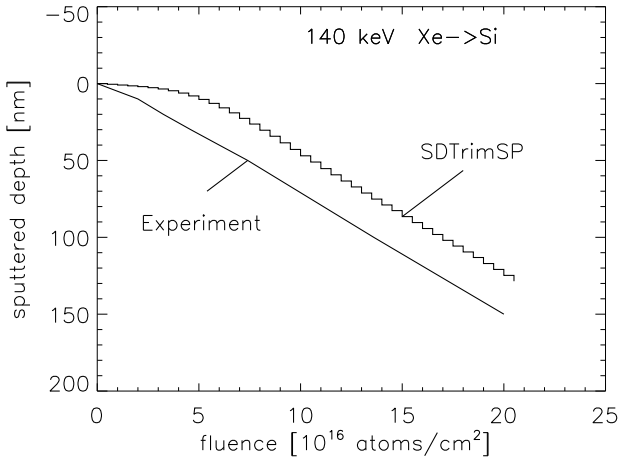

Fig. 4. Calculated sputtered depth for the bombardment of Si with 140 keV Xe at normal incidence compared with experimental data from [3]

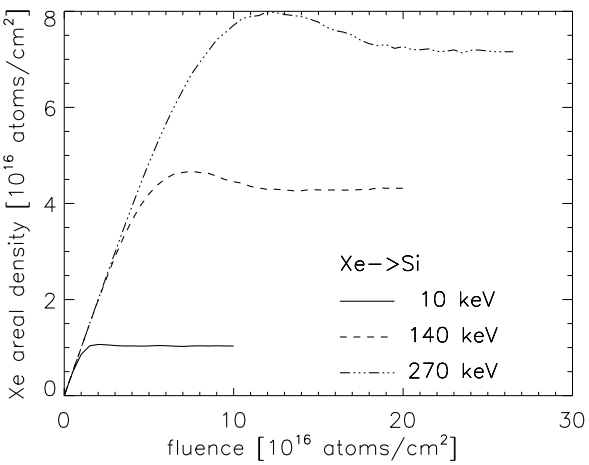

Fig. 5. Calculated areal density of implanted Xe versus the incident fluence. Si is bombarded with 10, 140 and 270 keV Xe at normal incidence

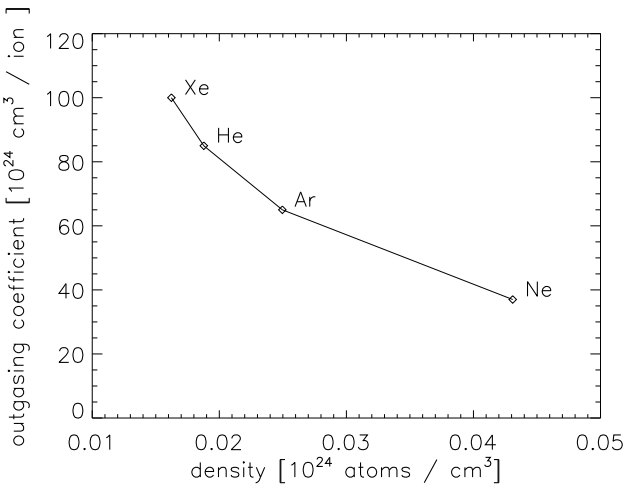

Fig. 6. Estimate of the outgasing coefficient, K, versus the liquid density of noble gases

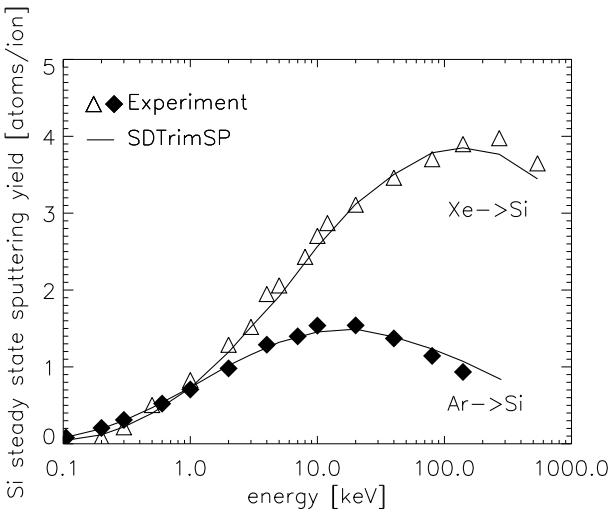

Fig. 7. Calculated steady state sputtering yields of Si versus the incident energy of Ar and Xe on a Si target at normal incidence compared with experimental data [9]

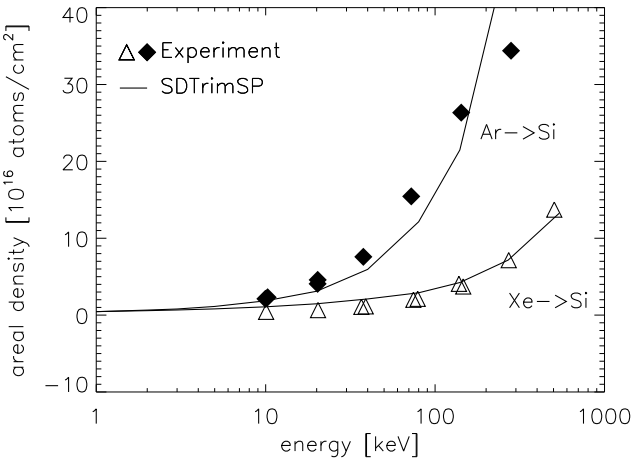

Fig. 8. Calculated steady state areal density of implanted Xe and Ar versus the incident energy of Ar and Xe on a Si target at normal incidence compared with experimental data [8]

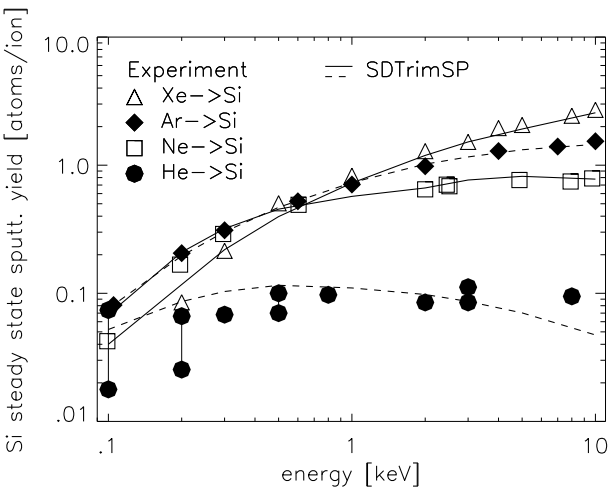

Fig. 9. Calculated steady state sputtering yields of Si versus the incident energy of He, Ne, Ar and Xe on a Si target at normal incidence compared with experimental data [9].

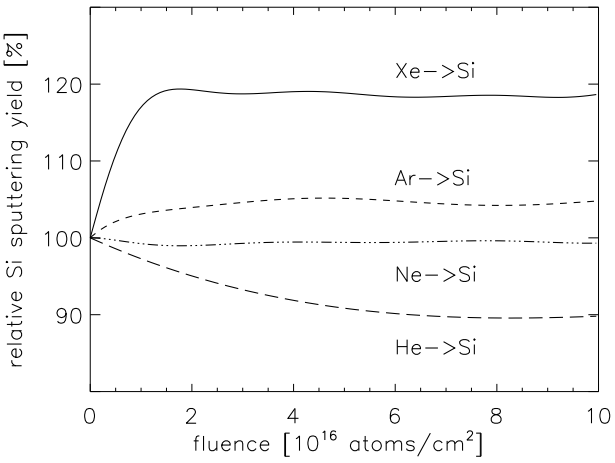

Fig. 10. Relative Si sputtering yields versus the incident fluence of 1 keV nobel gas on a Si target at normal incidence

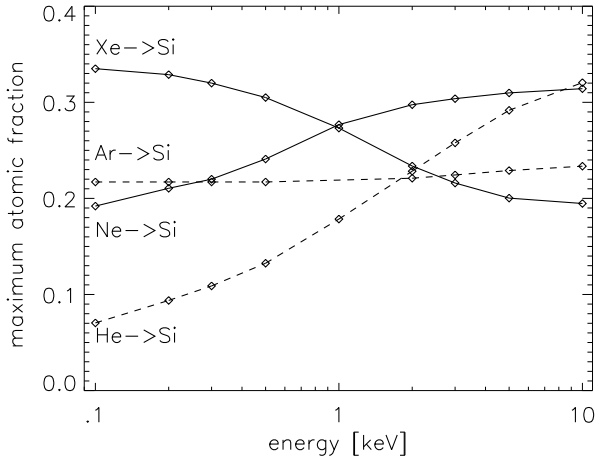

Fig. 11. Calculated steady state maximum atomic fractions of He, Ne, Ar, Xe in Si versus the incident energy at normal incidence. Lines are drawn to guide the eye

4 Conclusions

In general, the new program SDTrimSP that includes an outgassing procedure can well describe the fluence dependence of partial sputtering yields and the areal densities by noble gas bombardment of Si in good agreement with experimental data. The calculations provide new information beyond the experimental knowledge about the depth profiles of the implanted noble gas species He, Ne, Ar and Xe in Si with information about the maximum atomic fractions of these species in Si. The remaining smaller discrepancies between the model and experiment may be attributed to surface roughness induced by the ion bombardment. In the calculations a roughness only in atomic dimension is assumed.

In the program SDTrimSP, there is no attempt made to consider radiation damage as for example the creation of voids, clustering of implanted gases, or any inhomogeneity in density in the target. Although possible damage pro-

duced depends on energy and the mass ratio (damage highest for Ne and Ar on Si), the comparison between experimental and calculated data give no hints, that damage effects are of major importance.

The specific results of noble gas bombardment of Si apply also to other targets. If the mass ratio, A, of target mass to ion mass is distinctly different from unity, the steady state sputtering yield will be larger compared to low fluence bombardment if $A > 1$ and the opposite is true for $A < 1$. The available experimental data are overwhelmingly steady state values with an unknown amount of gas in the solid. Due to our calculated results the difference in the yields at low fluence and steady state will be smaller than 30% in most cases, depending on ion energy and angle of incidence. This difference is also relevant for a comparison between experimental data and results of static calculations.

5 Acknowledgements

The authors thank R. Behrisch, K. Schmid, and R. Schneider for reading of the manuscript and valuable discussions.

References

[1] W. Eckstein, J. Nucl. Mater. 281, (2000) 195

[2] W. Eckstein, Nucl. Instrum. Meth. B 171, (2000) 435

[3] P. Blank, K. Wittmaack, J. Appl. Phys. 50, (1979) 1519

[4] W. Eckstein, R. Dohmen, A. Mutzke, R. Schneider, Report IPP 12/3, Garching, (2007)

[5] J. P. Biersack, W. Eckstein, Appl. Phys. A 34, (1984) 73

[6] W. Eckstein, Computer Simulation of Ion-Solid Interactions, Springer Series in Material Science, Vol. 10, (Springer, Berlin, Heidelberg 1991)

[7] W. Eckstein, M. Hou, V.I. Shulga, Nucl. Instrum. Meth. B 119, (1996) 477

[8] P. Blank, K. Wittmaack, W. Wach, Radiat. Eff. 39, (1978) 81

[9] K. Wittmaack, Phys. Rev. B 68, 235211 (2003)